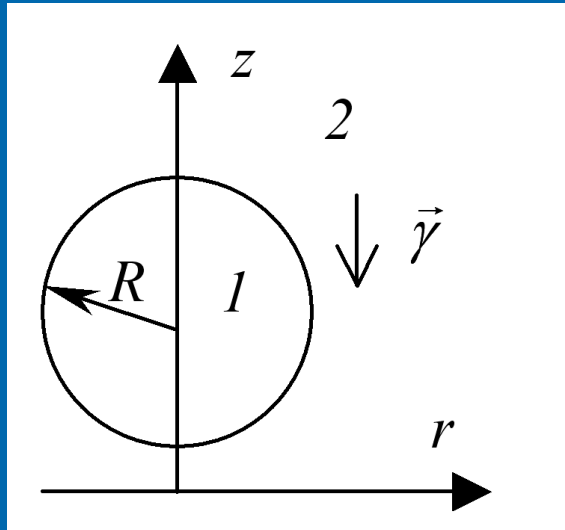


Effect of periodic forcing on stability of inclusion in porous media

Tatyana Lyubimova, Dmitriy Lyubimov,
Andrey Ivantsov

Perm State University, 614990, Perm, Russia
Institute of Continuous Media Mechanics UB RAS, 614013,
Perm, Russia

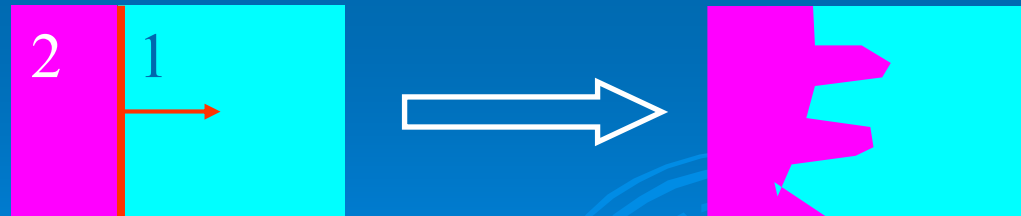
Problem statement



- The thickness of transitional layer between fluids where they are mixed is supposed to be small

➤ Instability of a displacement front

$$\frac{\eta_1}{K_1} > \frac{\eta_2}{K_2}$$



K. Aziz and A. Settari, Petroleum Reservoir Simulation, Applied Science, London (1979)

Numerical simulations drop sedimentation in porous medium

Darcy equation:

$$\nabla p + \frac{\eta}{k} \vec{u} = \rho g \vec{\gamma}$$

Governing equation in dimensionless form:

$$\nabla p + A \eta \vec{u} = \rho \vec{\gamma},$$

$$\text{where } A = \frac{\lambda - 1}{\mu + 0.5}$$

We use the following scales for variables:

$$[\rho] = \rho_1, \quad [\eta] = \eta_1, \quad [L] = R, \quad [u] = kg \frac{\rho_1 - \rho_2}{\eta_1 + 0.5\eta_2},$$

$$[t] = Kg \frac{\rho_1 - \rho_2}{\eta_1 + 0.5\eta_2} R, \quad [p] = \rho_1 g R.$$

Numerical simulations of drop sedimentation in porous medium

Dimensionless parameters are

$\lambda = \frac{\rho_2}{\rho_1}, \mu = \frac{\eta_2}{\eta_1}$ are dimensionless density and viscosity,

$r = \frac{\tilde{r}}{R}$ is drop radius

	$\eta, g / cm \cdot s$	$\rho, g / cm^3$	k, cm^2	ε
Water (1)	0,01	1,0	10^{-5}	0,3
Oil (2)	0,015	0,7		

Numerical algorithm:

- Level set method
- Adaptive mesh refinement
- Parallel computing

Level set method

According the approach two-phase system is represented as one media which parameters sharply changes across the interface

Density and viscosity are calculated by distance function:

$$\rho(\phi) = \lambda + (1 - \lambda)H(\phi)$$

$$\eta(\phi) = \mu + (1 - \mu)H(\phi)$$

$$H_{\varepsilon}(\phi) = \begin{cases} 0 & \text{if } \phi < -\varepsilon \\ \frac{1}{2} \left[1 + \frac{\phi}{\varepsilon} + \frac{1}{\pi} \sin(\pi\phi/\varepsilon) \right] & \text{if } |\phi| \leq \varepsilon \\ 1 & \text{if } \phi > \varepsilon \end{cases}$$

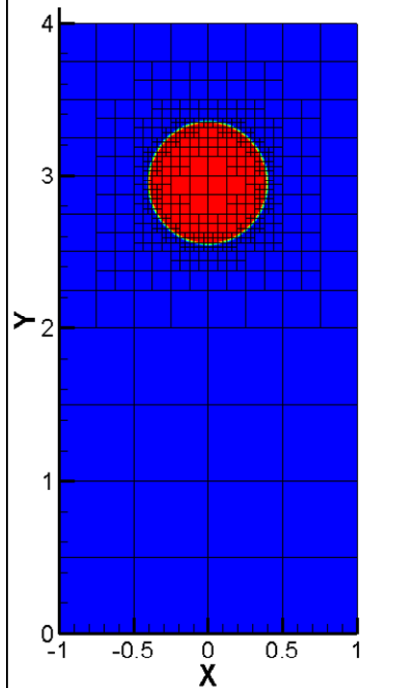
Calculations were perfumed for axisymmetric drop

$$v_z = -\frac{1}{r} \frac{\partial \psi}{\partial r}, \quad v_r = \frac{1}{r} \frac{\partial \psi}{\partial z}, \quad \Omega = \frac{\partial v_z}{\partial r} - \frac{\partial v_r}{\partial z}.$$

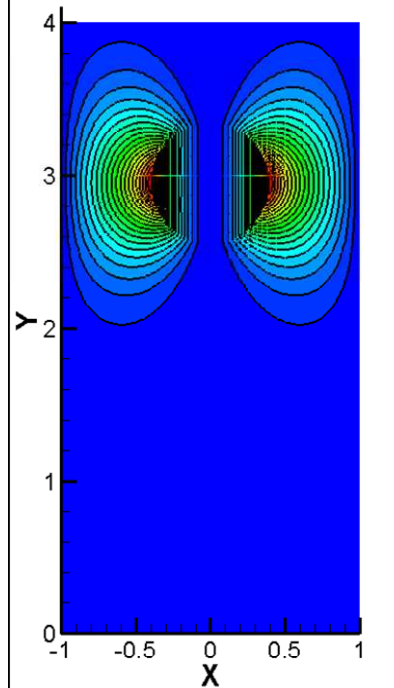
Adaptive mesh refinement

Parallel computing

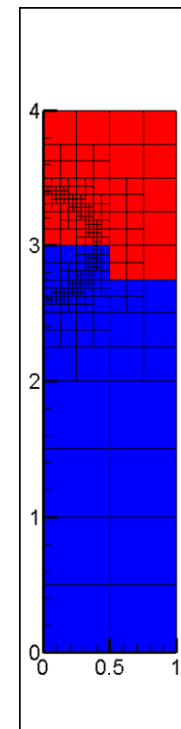
MacNeice P., Olson K.M., Mobarri C., Fainchtein R., Packer C. Paramesh: A parallel adaptive mesh refinement community toolkit // Computer Physics Communications. 2000. V.126. pp.330-354.



(a)



(b)

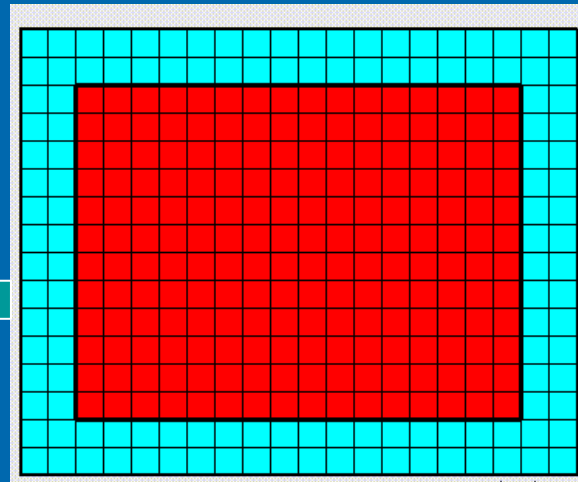
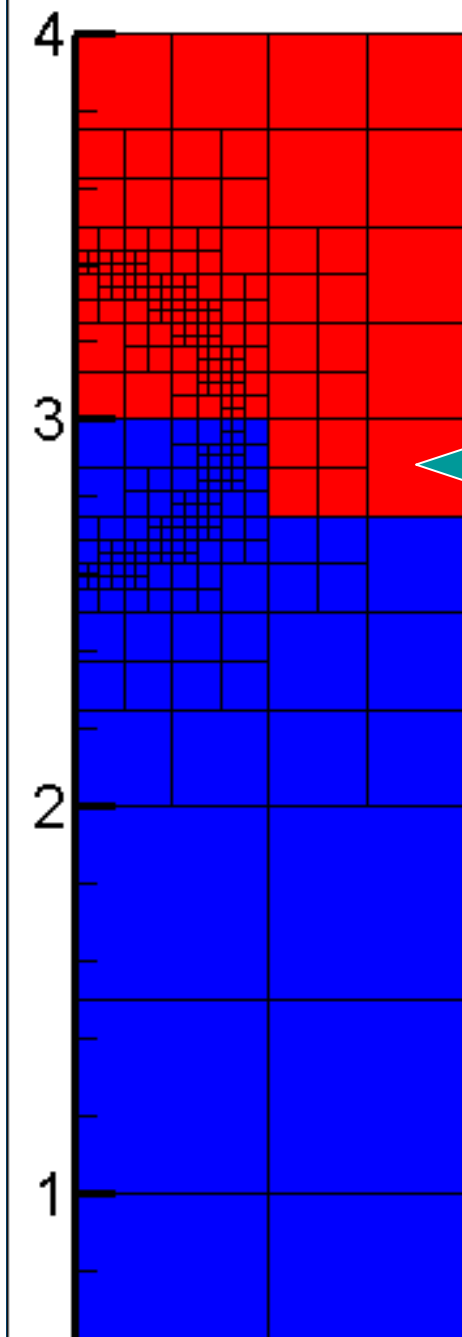


(c)

Axisymmetric drop sedimentation : (a) – initial drop shape and blocks of the mesh, (b) – flow function , (c) – distribution of mesh blocks among computation nodes

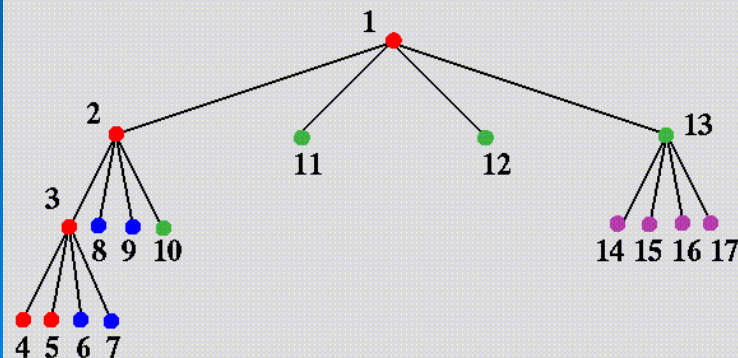
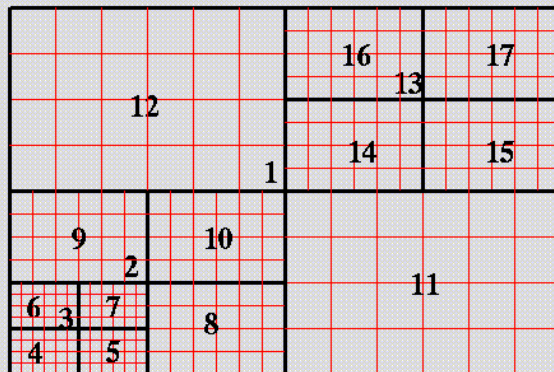
It is necessary to perform calculation with fine mesh near the interface

Mesh sub-grids



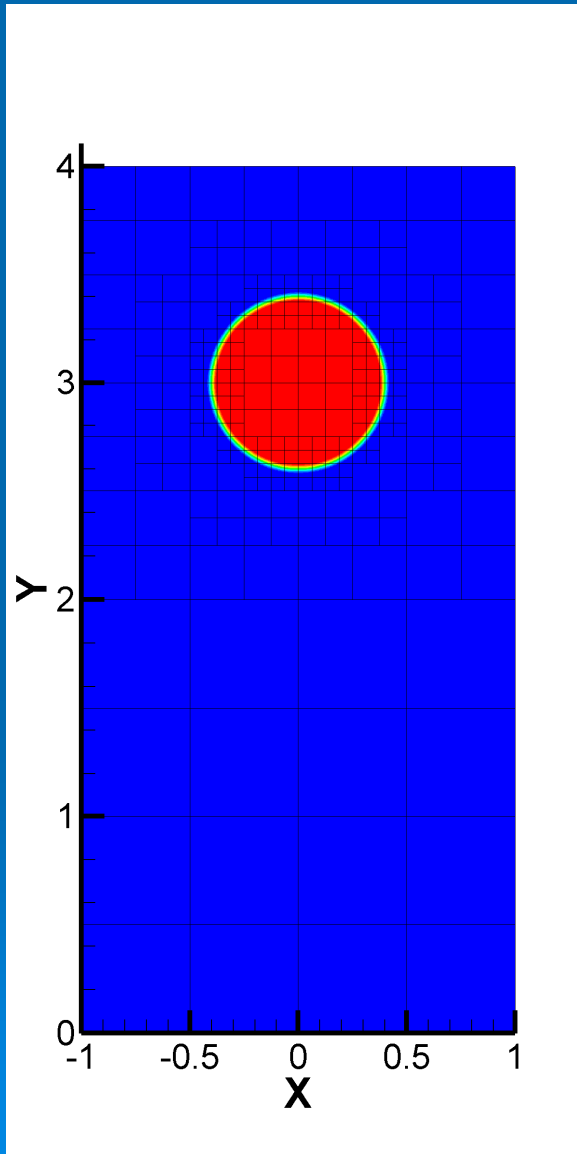
- The computational domain is covered with a hierarchy of numerical sub-grids.
- All the grid blocks have an identical logical structure. (ie the same number of grid points in each dimension, the same aspect ratios, the same number of guard cells, etc). They are assumed to be logically cartesian (or structured).

Hierarchy of sub-grids



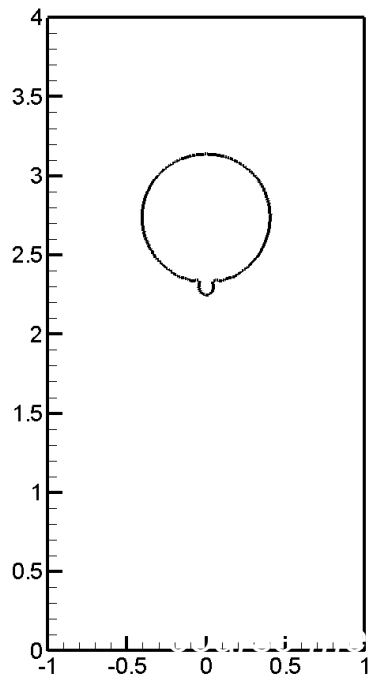
- The program builds a hierarchy of sub-grids to cover the computational domain, with spatial resolution varying to satisfy the demands of the application.
- These sub-grid blocks form the nodes of a tree data-structure.
- These sub-grids are distributed amongst the processors.

Results of computations

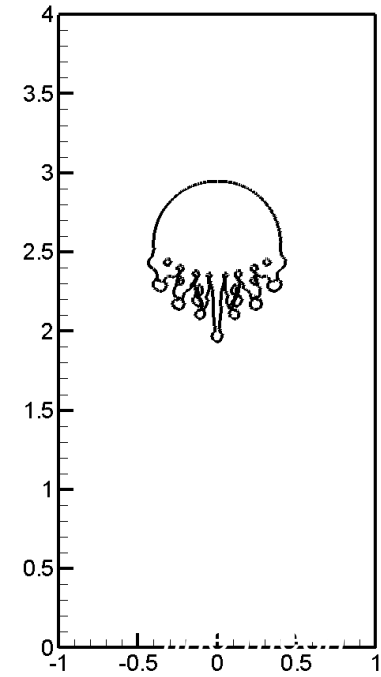
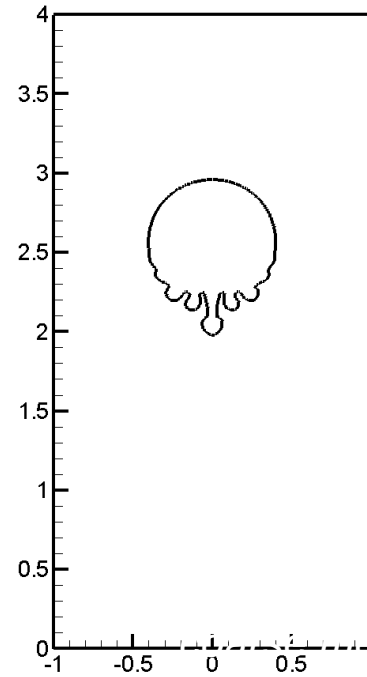
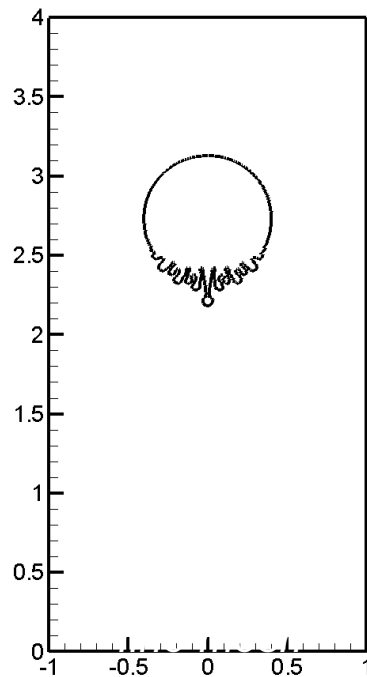


Water drop sedimentation
in porous medium saturated by oil

Numerical simulations drop sedimentation in porous medium



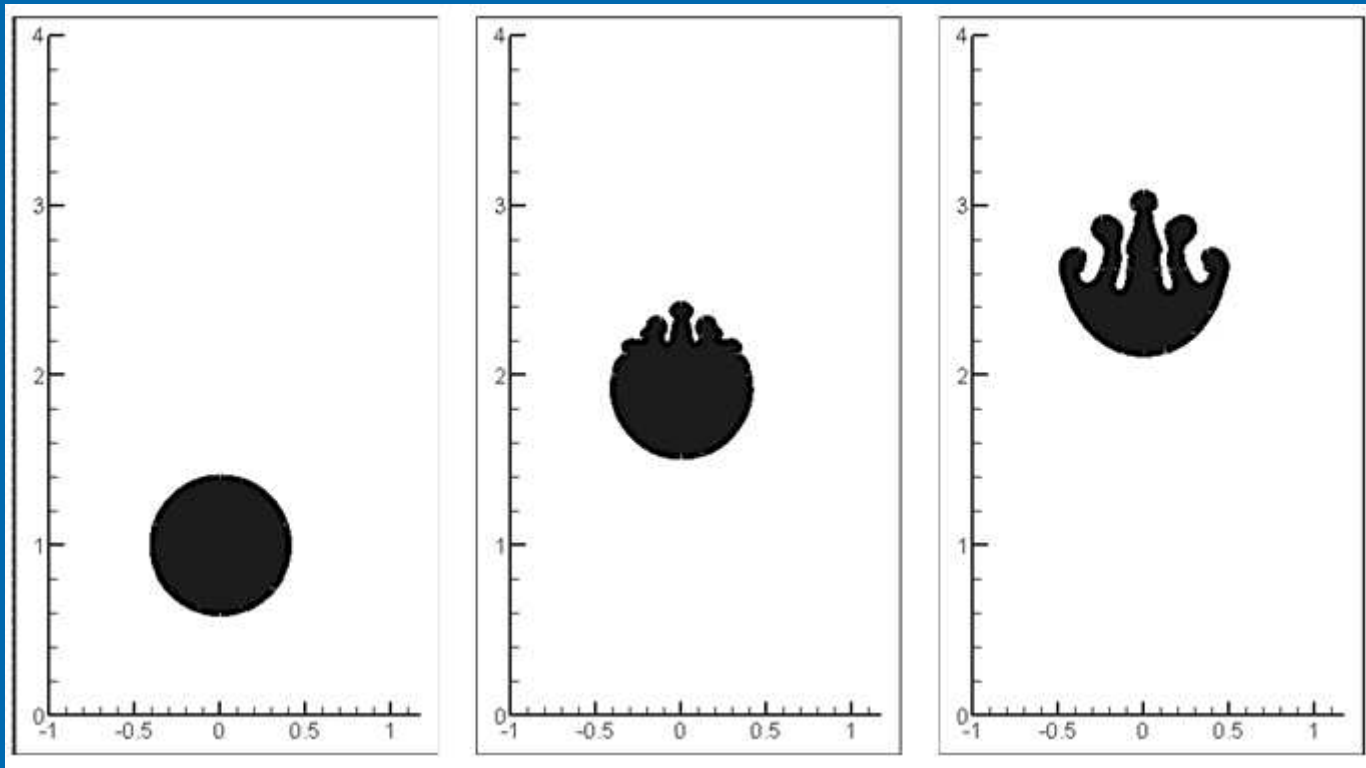
$t = 0.25$



$t = 0.5$

$$\lambda = 1.4 \quad \mu = 0.67 \quad r = 0.4$$

Emersion of oil drop in water



$t = 0$

$t = 1$

$t = 1.5$

$$\lambda = 1.4 \quad \mu = 0.67 \quad r = 0.4$$

Inclusion is instable. Perturbations of interface always grow at the front of moving inclusion

Part 2. Stability of inclusion under axial vibrations

Governing equations in dimensionless form:

$$\frac{\partial}{\partial t}(\rho \vec{u}) + (\vec{u} \nabla) \rho \vec{u} = -\nabla p - R \eta \vec{u} + \left(-\frac{1}{\text{Fr}} + a \cos t \right) \rho \vec{\gamma},$$
$$\text{div} \vec{u} = 0$$

$$[\rho] = \rho_1, \quad [\eta] = \eta_1, \quad [L] = R, \quad [u] = \varepsilon R \omega, \quad [t] = \frac{1}{\omega}, \quad [p] = \rho_1 R^2 \omega^2.$$

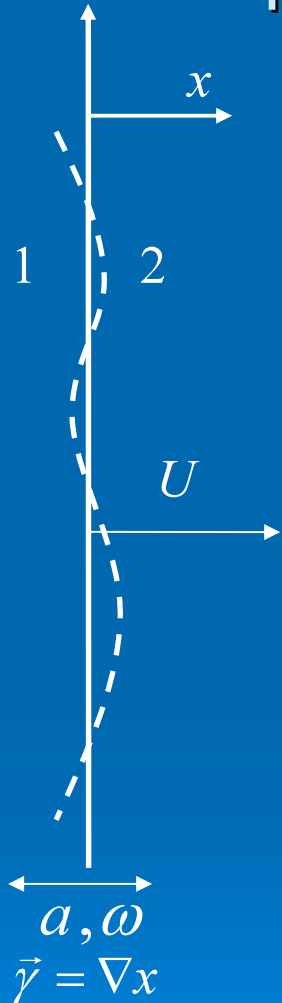
Dimensionless parameters:

$$R = \frac{\eta_1 \varepsilon}{\rho_1 k \omega} \text{ is dissipation parameter,} \quad \text{Fr} = \frac{R \omega^2}{g} \text{ is Froude number}$$

$$a = \frac{\tilde{a}}{R} \text{ is vibration amplitude}$$

High-frequency vibration effect on the displacement front stability in porous medium

D. V. Lyubimov and G. A. Sedel'nikov. Effect of Vibration on the Stability of a Plane Displacement Front in a Porous Medium. J. Fluid Dynamics, Vol. 41, No. 1, 2006, pp. 3–11.



$$\lambda_0 = -\frac{U}{\varepsilon} \frac{\eta_1 - \eta_2}{\eta_2 + \eta_1} k - \frac{2a^2 \omega^2 K (\rho_1 + \rho_2) (\rho_1 - \rho_2)^2}{\varepsilon (\eta_1 + \eta_2) [(\rho_1 + \rho_2)^2 + \varepsilon^2 (\eta_1 + \eta_2)^2 K^{-2} \omega^{-2}]} k^2$$

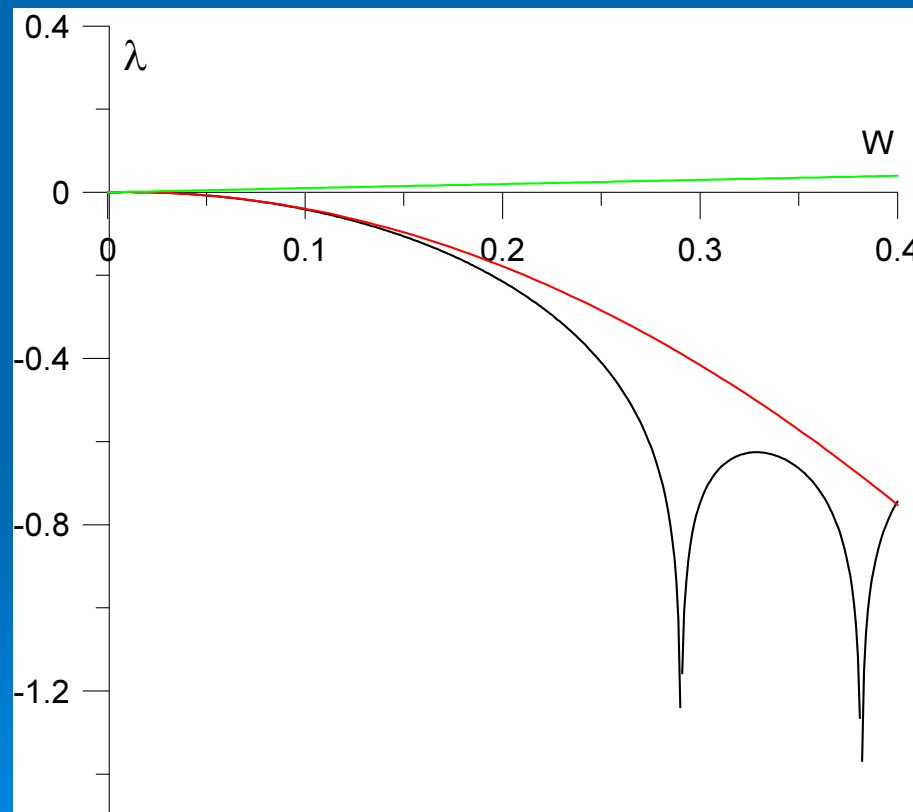
$$k_{cr} = \frac{U (\eta_2 - \eta_1) [(\rho_1 + \rho_2)^2 + \varepsilon^2 (\eta_1 + \eta_2)^2 K^{-2} \omega^{-2}]}{2a^2 \omega^2 K (\rho_1 + \rho_2) (\rho_1 - \rho_2)^2} \quad k' = k_{cr} / 2$$

$$T = \frac{2a^2 \omega^2 K \varepsilon (\eta_1 + \eta_2) (\rho_1 - \rho_2)^2}{U^2 (\eta_1 - \eta_2)^2 (\rho_1 + \rho_2) [1 + \varepsilon^2 (\eta_1 + \eta_2)^2 K^{-2} \omega^{-2} (\rho_1 + \rho_2)^{-2}]}$$

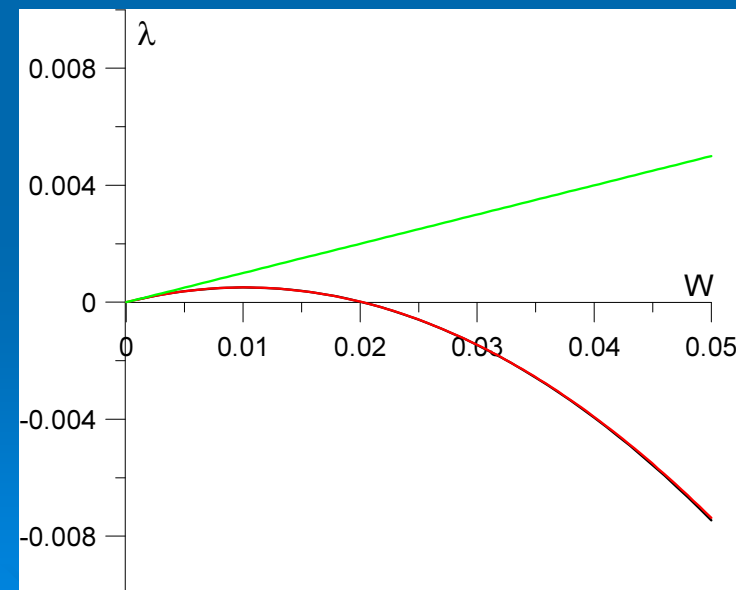
Finite frequency vibrations effect on the displacement front stability in porous medium

$$\ddot{B} + \sigma \dot{B} - W(1 + A \cos t) B = 0$$

$$\sigma = \frac{(\eta_1 + \eta_2)\varepsilon}{K(\rho_1 + \rho_2)\omega} = 0.7 \quad W = \frac{U(\eta_2 - \eta_1)k}{K(\rho_1 + \rho_2)\omega^2} = 3.7 \cdot 10^{-5} \cdot k(sm^{-1}) \quad A = \frac{a\omega^2(\rho_1 - \rho_2)K}{U(\eta_1 - \eta_2)} = 947.5$$

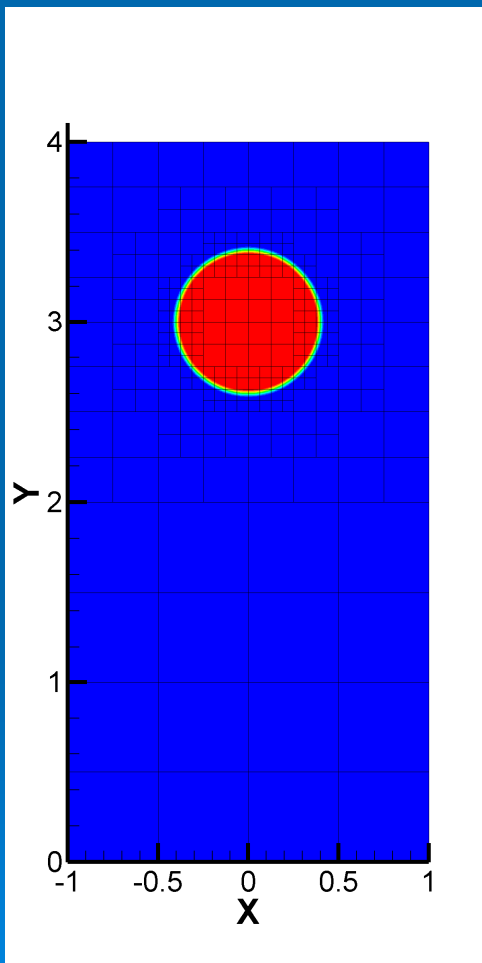


$$\sigma = 10 \quad A = 1000$$

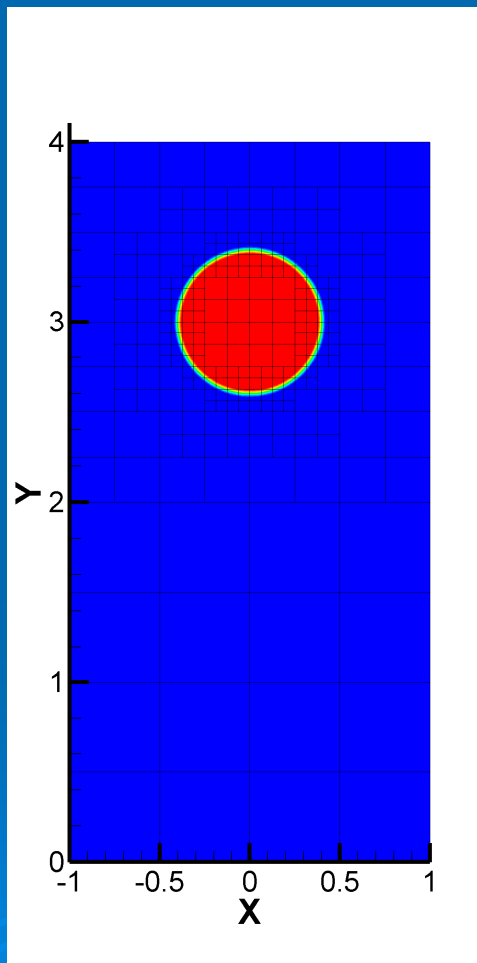


Sedimentation of water drop in porous medium saturated by oil under axial vibrations

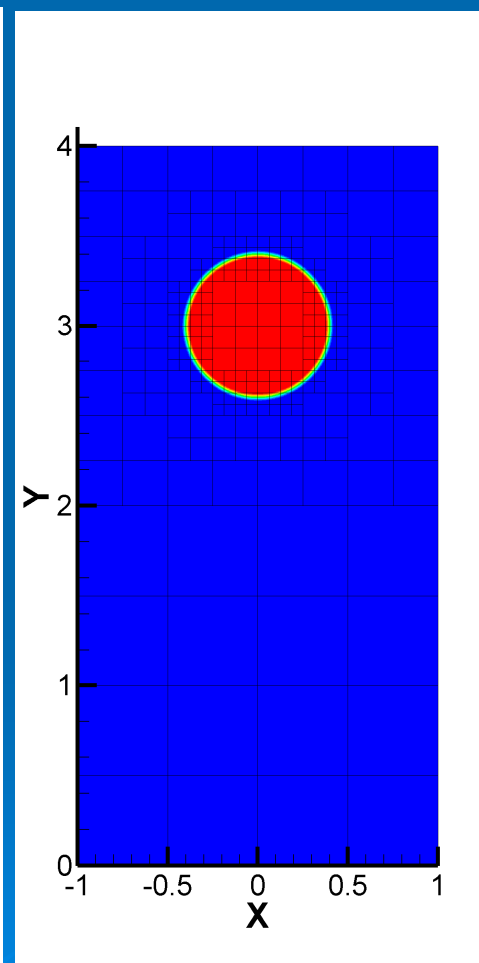
◆ Angular frequency eq. 100 1/c ◆ Chanel radius is 1 cm ◆ Drop radius is 0.4 cm



$a = 0.2$



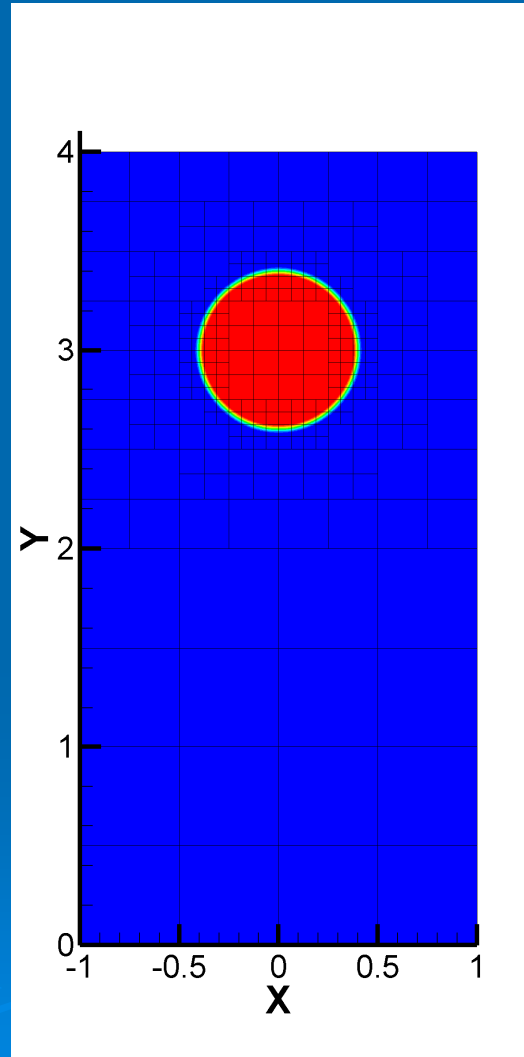
$a = 0.5$



$a = 1$

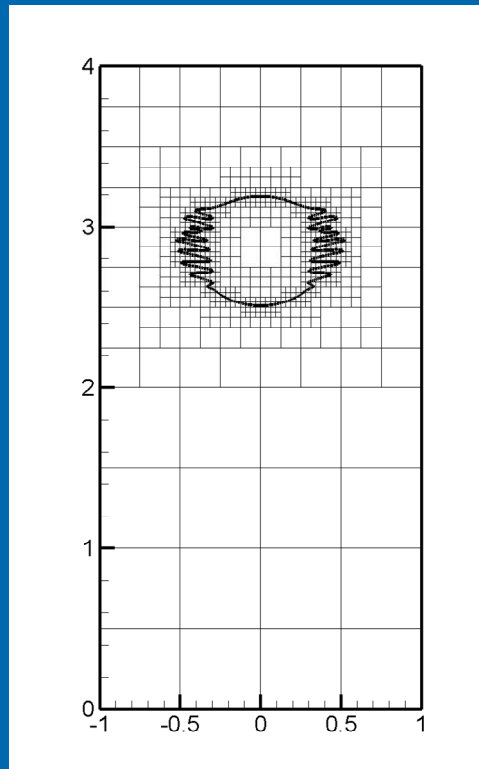
Sedimentation of water drop in porous medium saturated by oil under axial vibrations

$$\omega = 100 \text{ s}^{-1}$$
$$a = 2 \text{ cm}$$

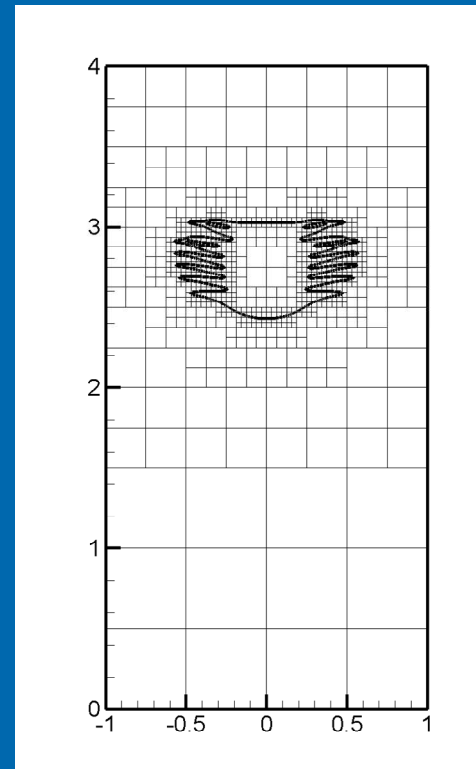


Sedimentation of water drop in porous medium saturated by oil under axial vibrations

$$\omega = 1000 \text{ s}^{-1}$$
$$a = 0.05 \text{ cm}$$

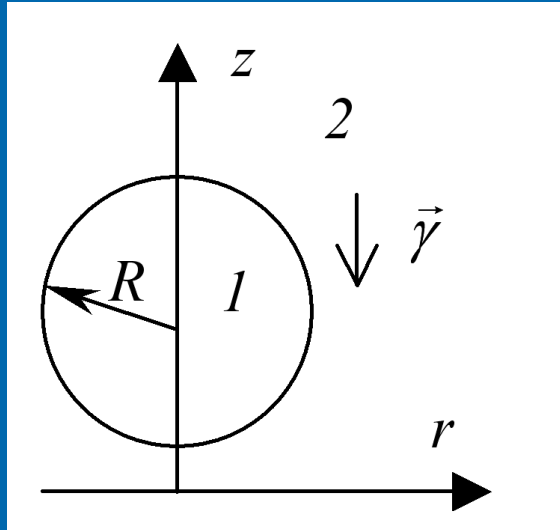


$t = 0.3 \text{ c.}$



$t = 0.65 \text{ c.}$

Part 3. Influence of modulated pumping



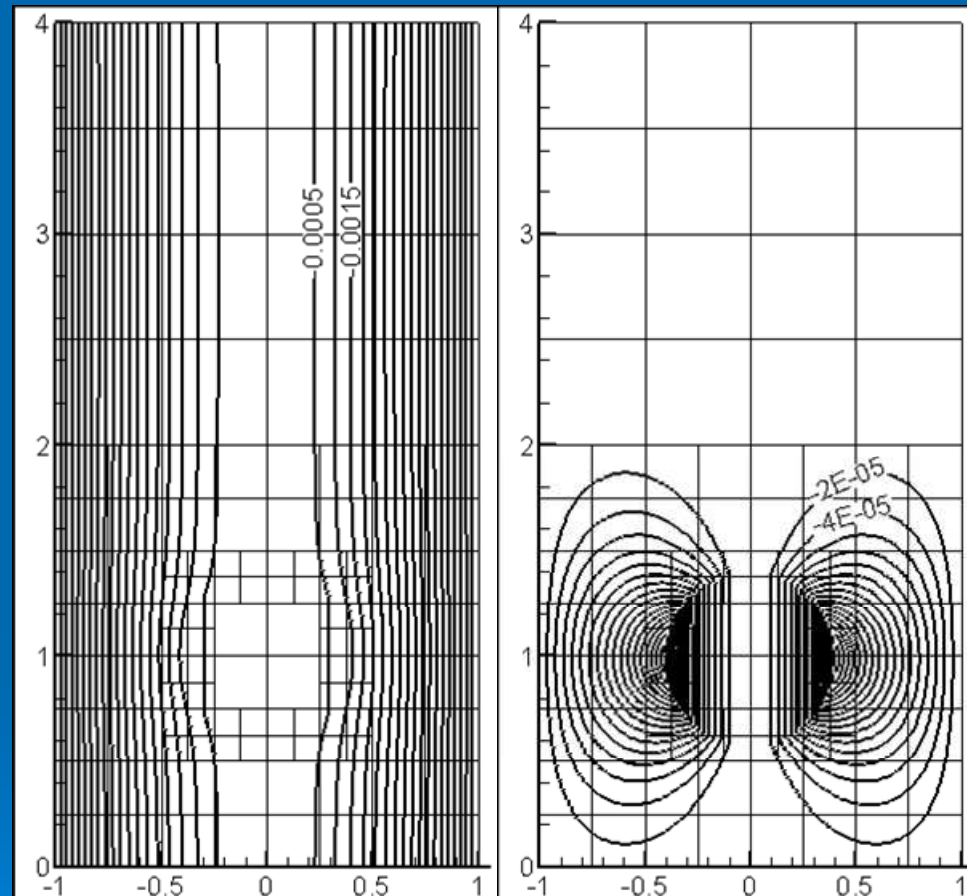
At upper and lower boundaries vertical component of velocity changes according the formula:

$$u_z = V \cos(\Omega t)$$

V is dimensionless velocity amplitude

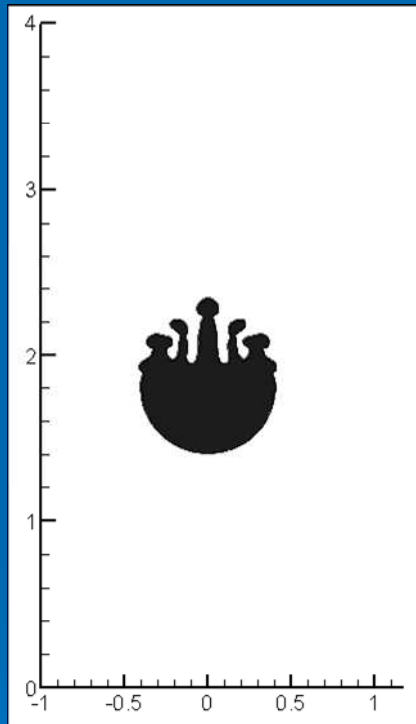
Ω is dimensionless frequency of external modulation.

Flow function

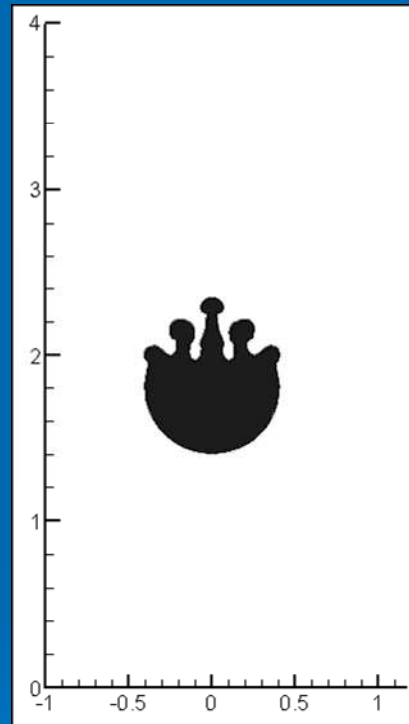


$$V = 0.02$$

Results



a

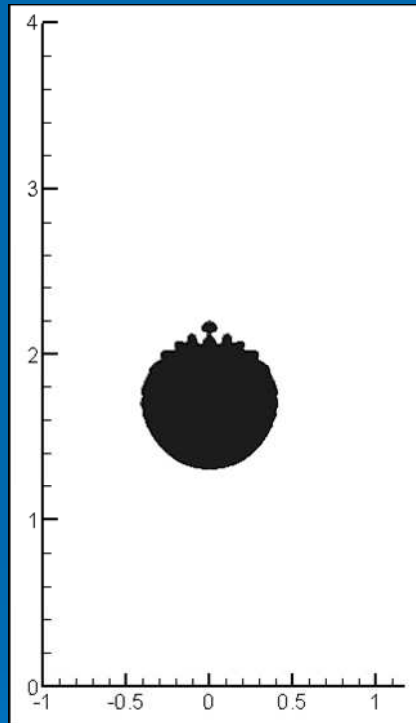


b

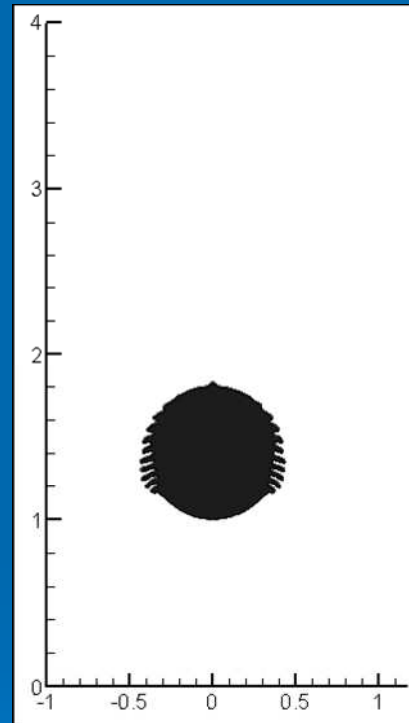
$V = 0.01, t = 15:$

a - $\Omega = 1$, b - $\Omega = 10$

Results



a



b

$\Omega = 10$:

a - $V = 0.02$, $t = 23$, b - $V = 0.03$, $t = 13$

Conclusions

Sedimentation or emersion of inclusion is instable. Perturbations of interface grow at the front of moving inclusion independently on viscosities values.

Vibrations can suppress short-wave perturbations of the displacement front, that are known to be most unstable (having the largest growth rate) in the classical non-vibrating case.

In the presence of weak vertical vibrations, similarly to the non-vibrating case, the droplet is unstable to small-scale perturbations localized near the front. Stronger vibrations can suppress the instability entirely.

Further increase of the strength of vibrations leads to another instability, this time localized at the droplet side.